Stars and their variability observed from space
C. Neiner, W. W. Weiss, D. Baade, R. E. Griffin, C. C. Lovekin, A. F. J. Moffat (eds)

UNBIASED SEISMIC MODEL FITTING

T. Kallinger[1]

Abstract. The unprecedented quality of data from space missions like Kepler and TESS enables detailed seismic studies of the interiors of many stars. However, such studies often require the computation of theoretical frequencies and the imperfect modelling of the star's near-surface layers introduces systematic uncertainties that hamper a direct comparison with the observations. To overcome this, various corrections have been introduced to reduce the systematic shifts between observed and model frequencies. Even though such corrections generally improve the analysis, they still bear unpredictable systematics and therefore prevent us from making the best use of the observations. I present here a new approach that uses probabilistic methods to marginalise the surface effect. This therefore enables an unbiased search for a best-fit model by using only the observed frequencies and without the need to correct for the surface effect. The approach is tested with Kepler data of the red giant component in the eclipsing binary system KIC 8410637 and gives accurate stellar fundamental parameters that are in agreement with independent measurements.

Keywords: stars: late-type – stars: oscillations (including pulsations) – stars: fundamental parameters – stars: solar-type – stars: individual: KIC 8410637

1 Introduction

Asteroseismology is a major part of the space photometry revolution. The detection of solar-type oscillations in hundreds of sun-like stars and thousands of evolved cool giants has triggered many breakthroughs in stellar astrophysics (e.g. Bedding et al. 2011; Beck et al. 2012; Kallinger et al. 2010b). The availability of photometric time-series data of unprecedented duration and quality should enable precise determination of both the global stellar parameters and interiors by comparing the observed oscillations to the eigen-frequencies of stellar models.

However, such an approach still suffers from uncertainties in the models, like the insufficient treatment of convection. The resulting systematic shifts in the theoretical frequencies complicate a direct comparison between observed and model frequencies. This so-called seismic surface effect was first recognised for the Sun (e.g. Brown 1984) and has since been extensively investigated (e.g. Houdek et al. 2017). Lacking a definitive conclusion, Kjeldsen et al. (2008) proposed to empirically model the surface effects as a power law in frequency. They calibrated the power-law exponent to the difference between the observed solar frequencies and theoretical frequencies computed from a standard solar model. Such a correction is indeed required to avoid matching the observed frequencies to a model with systematically incorrect properties and interior structure. However, their correction over-estimates the effect at low frequencies and assumes that the frequency shifts follow the same power law in all stars.

Ball & Gizon (2014) proposed to model the surface effect as a combination of an inverse and cubic frequency term normalised by the mode inertia, which does not rely on a solar calibration. This improved the correction for the Sun but is likely also not universally applicable. In fact, Gruberbauer et al. (2013) showed that the surface effect significantly varies across the HR-diagram and Sonoi et al. (2015) argued that instead of calibrating it to the Sun, the surface corrections should be constrained from realistic physical modelling as provided by 3D hydrodynamical simulations.

Even though standard surface corrections have extensively been used (e.g. Mathur et al. 2012) it is not yet understood if they are actually applicable for stars different from the Sun. To verify this is quite difficult as one needs accurate independent measurements for the stellar properties, which are usually not available for the mostly faint stars targeted by photometric space missions like *Kepler*. Rare exceptions are eclipsing binary systems with at least one oscillatory component, for which precise and accurate dynamic masses and radii can be determined from radial velocity and photometric eclipse observations (e.g. Gaulme et al. 2016). Ball et al. (2018) investigated three such systems with a red giant component and found that none of the available surface corrections are sufficient to seismically model the stars in agreement with the dynamic parameters.

[1] Institut für Astrophysik, Universität Wien, Türkenschanzstrasse 17, 1180 Vienna, Austria

Here, I introduce a new method that allows for unbiased seismic forward modelling without the need to explicitly correct the model frequencies for the surface effect. The method defines the search for a match between a set of observed and the corresponding model frequencies in a Bayesian framework. It thereby introduces an additional frequency offset parameter, which is then marginalised without the need to explicitly know its value.

2 Bayesian asteroseismic forward modelling

In seismic forward modelling the search for a best fit is usually quantified by minimising the sum of the squared differences between the observed and model frequencies. However, to consistently encode possibly available prior information and to make use of all advantages that come with Bayesian statistics it is more convenient to perform the model fitting in a probabilistic framework. Kallinger et al. (2010a) formulated asteroseismic model fitting in terms of Bayes' theorem,

$$p(\mathcal{M}|\mathcal{D},\mathcal{I}) = \frac{p(\mathcal{M}|\mathcal{I}) \cdot p(\mathcal{D}|\mathcal{M},\mathcal{I})}{p(\mathcal{D},\mathcal{I})}. \tag{2.1}$$

The prior probability $p(\mathcal{M}|\mathcal{I})$ is for a specific model ($\mathcal{M}$) for which one can encode prior information ($\mathcal{I}$) on, e.g., the fundamental parameters of the star. The likelihood function,

$$p(\mathcal{D}|\mathcal{M},\mathcal{I}) = \prod_{\mathrm{i}}^{N_{\mathrm{obs}}} \frac{1}{\sigma_{\mathrm{i}}\sqrt{2\pi}} \exp\left(\frac{-(\nu_{\mathrm{i,obs}} - \nu_{\mathrm{i,mod}})^2}{2\sigma_{\mathrm{i}}^2}\right), \tag{2.2}$$

combines the probability that a given model frequency ν_{mod} matches an observed frequency ν_{obs}, which follows from the Gaussian distribution of the uncertainties $\sigma^2 = \sigma_{\mathrm{obs}}^2 + \sigma_{\mathrm{mod}}^2$. The denominator in Eq. 2.1 is a normalisation factor for the specific model probability in the form of $p(\mathcal{D},\mathcal{I}) = \sum_{\mathrm{i}} p(\mathcal{M}_{\mathrm{i}}|\mathcal{I}) \cdot p(\mathcal{D}|\mathcal{M}_{\mathrm{i}},\mathcal{I})$. By maximising Eq. 2.1 one can identify a best match between the observed and model frequencies and determine the best-fit model parameters and their uncertainties from the marginal distribution of the corresponding parameter.

Even though the Bayesian approach allows for a realistic error determination and statistically correct comparison of different solutions, it still suffers (in its current form) from systematic errors in the model frequencies. However, one of the major strengths of the probabilistic framework is the marginalisation of model parameters. Any parameter θ, needed to describe a model, can be marginalised by applying the sum rule of probability theory (Jaynes ????), which in the case of continuous parameters, turns into an integral. By integrating the full posterior over the parameter range of θ, one obtains the marginal posterior that still retains the overall effects of including θ in the model, but is independent of any particular choice of its value.

Gruberbauer et al. (2012) have shown that this "Bayesian trick" can perfectly be applied to the unknown systematic errors in seismic model fitting. They showed that, if Δ_{i} is the systematic shift of an individual model frequency, Eq. 2.2 can be modified as

$$p(\mathcal{D}|\mathcal{M},\mathcal{I}) = \prod_{\mathrm{i}}^{N_{\mathrm{obs}}} \int_{\Delta_{\mathrm{i,min}}}^{\Delta_{\mathrm{i,max}}} p(\Delta_{\mathrm{i}}|\mathcal{I}) \times \frac{1}{\sigma_{\mathrm{i}}\sqrt{2\pi}} \exp\left(\frac{-(\nu_{\mathrm{i,obs}} - \nu_{\mathrm{i,mod}} - \Delta_{\mathrm{i}})^2}{2\sigma_{\mathrm{i}}^2}\right) d\Delta_{\mathrm{i}}, \tag{2.3}$$

to marginalise (i.e., to remove) the influence of the surface effect in the model search. Even though Δ_{i} remains an unknown parameter, its influence is fully considered in the probabilistic analysis as long as its upper and lower boundaries can be roughly estimated. Here, $p(\Delta|\mathcal{I})$ encodes prior information about the expected behaviour of the surface effect, with $\int p(\Delta_{\mathrm{i}}|\mathcal{I}) d\Delta_{\mathrm{i}} = 1$. Gruberbauer et al. (2012) suggested a parameter-free beta prior $p(\Delta_{\mathrm{i}}|\mathcal{I}) = 2(\Delta_{\mathrm{i,max}} - \Delta_{\mathrm{i}})/\Delta_{\mathrm{i,max}}^2$, leading to a linearly decreasing probability density with the advantage of being properly normalised, and of reaching zero at $\Delta_{\mathrm{i}} = \Delta_{\mathrm{i,max}}$. Finally, $\Delta_{\mathrm{i,min}}$ is set to zero and $\Delta_{\mathrm{i,max}} = a \cdot \Delta\nu \left(\nu_{\mathrm{i,obs}}/\nu_{\mathrm{max}}\right)^b$, where a and b are fixed to 0.3 and 4.9, respectively. In fact, the latter are not very critical as long as it is ensured that the real Δ_{i} is covered by the range. Similar values of a and b or even a different functional form of $\Delta_{\mathrm{i,max}}$ (e.g., a Lorentzian) give similar results.

The above-described surface-correction independent approach correctly identifies the mean density of a star but has only low discriminative power to disentangle its mass and radius (see Fig. 1a). This is not surprising since the marginalisation of Δ_{i} gives similar weight to a relatively broad range of models. Gruberbauer et al. (2013) overcame this problem by encoding prior information about the star's fundamental parameters. However, this should be avoided, since the model's $M - L - T_{\mathrm{eff}}$ relation very much depends on the adopted mixing length parameter and primordial chemical composition, and is therefore highly model-dependent. Instead, I aim to constrain the models by using *only* the observed frequencies.

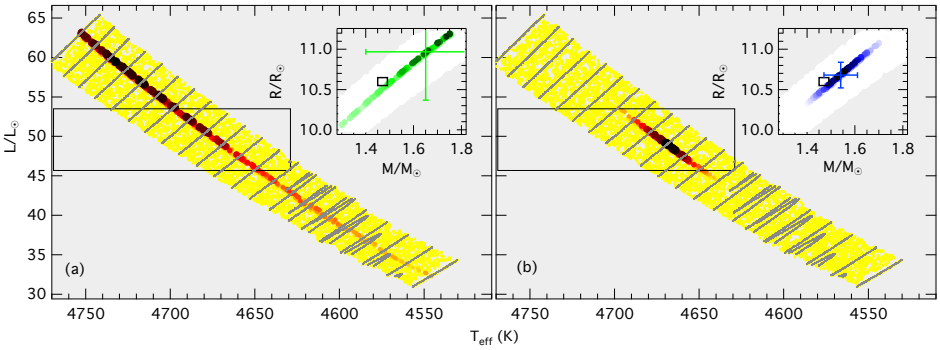

Fig. 1. HR diagram showing the uncertainty box of KIC 8410637 and a subset of the stellar model grid used to fit the observed frequencies. Grey dots indicate the original grid and colored dots are interpolated models with the color scale indicating the goodness of the fit (the darker the better). Panels (b) and (c) show posterior model probabilities from the surface-correction independent Bayesian forward modelling based on Eq. 2.3 and 2.5, respectively. Inserts show the same in the $M - R$ plane and the corresponding best-fit values and uncertainties. The black error box shows the dynamic solution from Themeßl et al. (2018).

It is well-known that periodic deviations from the regular mode pattern are the signature of acoustic glitches (e.g. Gough 1990) due to sharp structural variations in the stellar interior. While the modulation period is related to the sound-travel time from the structural feature to the stellar surface, its amplitude depends on the width of the glitch. In red giants, the main source of observable discontinuities is the 2nd helium ionisation zone, and Miglio et al. (2010) found that its relative acoustic radius varies with mass (in their models). It should therefore be possible to use the glitch signal to disentangle the mass and radius in the above fit.

Apart from the glitch signal, the oscillation modes of a red giant are also modulated by the so-called curvature, which can be described by a second-order development of the asymptotic theory and is presumably due to hydrogen ionisation just below the stellar surface. To disentangle the glitch and curvature signal in the observed and model frequencies (which also contain a modulation from the surface effect!), I follow Kallinger et al. (2018) and compute a second-order polynomial fit and subtract it from the original frequencies as,

$$\nu'(n) = \nu(n) - \left[\nu_{\rm c} + \Delta\nu_{\rm cor}\left(n - n_{\rm c} + \frac{\alpha}{2}(n - n_{\rm c})^2\right)\right], \tag{2.4}$$

where $\nu_{\rm c}$ and $n_{\rm c}$ are the frequency and radial order of the central radial mode, respectively, α is the curvature parameter, and $\Delta\nu_{\rm cor}$ the curvature-corrected large separation. One can now add a term to Eq. 2.3,

$$p(\mathcal{D}|\mathcal{M},\mathcal{I}) = \prod_{\rm i}^{N_{\rm obs}} \int_{\Delta_{\rm i,min}}^{\Delta_{\rm i,max}} \frac{p(\Delta_{\rm i}|\mathcal{I})}{\sigma_{\rm i}\sqrt{2\pi}} \exp\left(\frac{-(\nu_{\rm i,obs} - \nu_{\rm i,mod} - \gamma\Delta_{\rm i})^2}{2\sigma_{\rm i}^2}\right) d\Delta_{\rm i} \frac{1}{\sigma'_{\rm i}\sqrt{2\pi}} \exp\left(\frac{-(\nu'_{\rm i,obs} - \nu'_{\rm i,mod})^2}{2\sigma_{\rm i}'^2}\right), \tag{2.5}$$

which also compares the glitch contributions of the observed and model frequencies, where the uncertainties σ' result from Eq. 2.4.

3 The test case KIC 8410637 and conclusions

To demonstrate the abilities of the Bayesian asteroseismic forward modelling I use the *Kepler* data of KIC 8410637, which is a detached eclipsing binary system consisting of a RGB and MS component, that circle each other in a 408-day orbit (Hekker et al. 2010; Frandsen et al. 2013). Themeßl et al. (2018) determined the mass and radius of the RGB component to be $1.47 \pm 0.02\,{\rm M}_\odot$ and $10.60 \pm 0.05\,{\rm R}_\odot$, respectively, and found the system to have a near solar chemical composition. The photometry of KIC 8410637 reveals a clear red-giant oscillation spectrum, which makes the system an ideal target for testing various asteroseismic applications, (Kallinger et al. 2018; Ball et al. 2018; Li et al. 2018; Buldgen et al. 2019). To extract the mode frequencies from the *Kepler* data I follow the approach of Kallinger (2019) and determine a sequence of six consecutive radial modes with frequencies in agreement with the measurements of Themeßl et al. (2018) and Li et al. (2018).

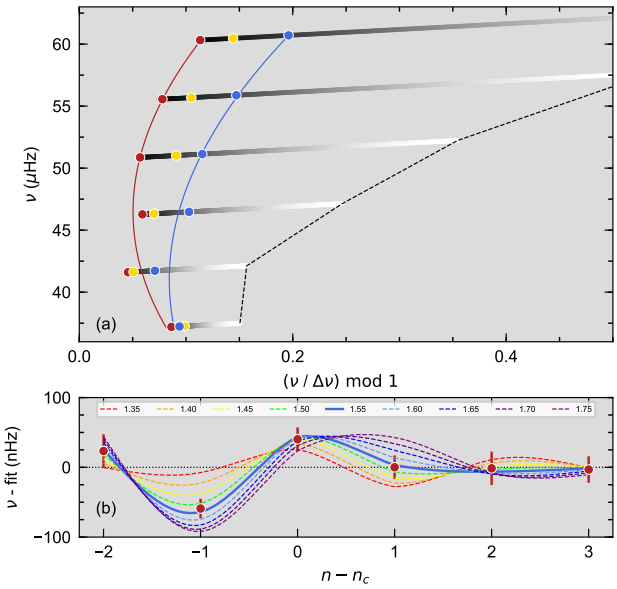

Fig. 2. Echelle diagram of KIC 8410637. Panel (a) shows the observed (red symbols) and best-fit model frequencies, where yellow and blue symbols correspond to fits based on Eq. 2.3 and 2.5, respectively. Red and blue lines give second-order polynomial fits to the frequencies (i.e. curvature). The grey-shaded trails indicate the prior probability density for varying $\Delta_{\rm i}$, with black and white corresponding to a probability of one and zero, respectively. The dashed line gives $\Delta_{\rm i,max}$. Panel (b) gives the curvature-corrected observed frequenices and a sequence of models (colored lines), where instead of the actual model frequencies, spline fits are shown for better visibility.

The stellar models used in this analysis are computed with `MESA`* (Paxton et al. 2011) for an initial chemical composition of (Y, Z) = (0.286, 0.023) and $\alpha_{\rm MLT} = 2.1$ and cover a mass ranging from 1 to $2\,{\rm M}_\odot$ in steps of $0.05\,{\rm M}_\odot$ from the early giant branch ($\log g \leq 3.4$) to after the core-He burning phase. Overshooting and mass loss are turned off. Adiabatic mode frequencies for the roughly 110 000 RGB and post-RGB models are then computed with the `GYRE`† stellar oscillation code (Townsend & Teitler 2013), using an outer mechanical boundary condition as described by Christensen-Dalsgaard (2008).

A fit to the observed frequencies based on Eq. 2.3 results in a precise mean stellar density of $1.260 \pm 0.006 \times 10^{-3} \rho_\odot$, which is also in good agreement with the dynamic solution. The mass and radius are, however, only poorly constrained and in principle overestimated in comparison to the dynamic values (see Fig. 1a). Considering also the glitch signal (fit based on Eq. 2.5) significantly changes the situation and reveals a much better defined mass and radius of $1.54 \pm 0.07\,{\rm M}_\odot$ and $10.68 \pm 0.17\,{\rm R}_\odot$, respectively (see Fig. 1b), which agree to within -5 ± 5 and $0.7 \pm 1.6\%$ with the dynamic measurements of Themeßl et al. (2018). The observed and best-fit model frequencies are illustrated in Fig. 2. As a byproduct, the fit also allows one to quantify the actual surface effect of the best-fit model frequencies, which is inconsistent with predictions from the widely used surface corrections of Kjeldsen et al. (2008) and Ball & Gizon (2014). More details about this are, however, beyond the scope of this proceedings paper and will soon be presented in a separate article (Kallinger, A&A submitted).

References

Ball, W. H. & Gizon, L. 2014, A&A, 568, A123

Ball, W. H., Themeßl, N., & Hekker, S. 2018, MNRAS, 478, 4697

Beck, P. G., Montalban, J., Kallinger, T., et al. 2012, Nature, 481, 55

Bedding, T. R., Mosser, B., Huber, D., et al. 2011, Nature, 471, 608

Brown, T. M. 1984, Science, 226, 687

Buldgen, G., Rendle, B., Sonoi, T., et al. 2019, MNRAS, 482, 2305

*http://mesa.sourceforge.net

†https://bitbucket.org/rhdtownsend/gyre/wiki/Home

Christensen-Dalsgaard, J. 2008, Ap&SS, 316, 113

Frandsen, S., Lehmann, H., Hekker, S., et al. 2013, A&A, 556, A138

Gaulme, P., McKeever, J., Jackiewicz, J., et al. 2016, ApJ, 832, 121

Gough, D. O. 1990, in Lecture Notes in Physics, Berlin Springer Verlag, Vol. 367, Progress of Seismology of the Sun and Stars, ed. Y. Osaki & H. Shibahashi, 283

Gruberbauer, M., Guenther, D. B., & Kallinger, T. 2012, ApJ, 749, 109

Gruberbauer, M., Guenther, D. B., MacLeod, K., & Kallinger, T. 2013, MNRAS, 435, 242

Hekker, S., Debosscher, J., Huber, D., et al. 2010, ApJ, 713, L187

Houdek, G., Trampedach, R., Aarslev, M. J., & Christensen-Dalsgaard, J. 2017, MNRAS, 464, L124

Jaynes, E. T. ???? (Cambridge: Cambridge University Press, timestamp = 2011-05-10T10:42:42.000+0200, title = Probability theory: The logic of science, year = 2003)

Kallinger, T. 2019, arXiv e-prints, arXiv:1906.09428

Kallinger, T., Beck, P. G., Stello, D., & Garcia, R. A. 2018, A&A, 616, A104

Kallinger, T., Gruberbauer, M., Guenther, D. B., Fossati, L., & Weiss, W. W. 2010a, A&A, 510, A106

Kallinger, T., Mosser, B., Hekker, S., et al. 2010b, A&A, 522, A1

Kjeldsen, H., Bedding, T. R., & Christensen-Dalsgaard, J. 2008, ApJ, 683, L175

Li, T., Bedding, T. R., Huber, D., et al. 2018, MNRAS, 475, 981

Mathur, S., Metcalfe, T. S., Woitaszek, M., et al. 2012, ApJ, 749, 152

Miglio, A., Montalbán, J., Carrier, F., et al. 2010, A&A, 520, L6

Paxton, B., Bildsten, L., Dotter, A., et al. 2011, ApJS, 192, 3

Sonoi, T., Samadi, R., Belkacem, K., et al. 2015, A&A, 583, A112

Themeßl, N., Hekker, S., Southworth, J., et al. 2018, MNRAS, 478, 4669

Townsend, R. H. D. & Teitler, S. A. 2013, MNRAS, 435, 3406